Journal of Transportation System and Engineering, Vol.2
ISSN: 3059-9865(Print) 3059-9873(Online)
Volume 2, Issue 1 2026 (July):
DOI: https://doi.org/10.3126/jotse.v2i1.97153
Society of Transport Engineers Nepal (SOTEN)

Research Article
Received Date:04/12/2026
Accepted Date:05/22/2026
Published Date:07/14/2026

Catalogue for Geosynthetically Stabilized Road Pavements Using 3D Finite Element Analysis

Aanchal Tiwari[a,*], Ram Chandra Tiwari[b,*], Prabhat Kumar Jha[c], Dhanapati Dhakal[d], Bijaya Bhusal[e], Kabin Lamichhane[f], Bijaya Bhattarai[g], Diwas KC[h]

M.Sc. in Transportation Engineering, Department of Civil Engineering, Pulchowk Campus, Institute of engineering, Tribhuvan University, Lalitpur, 44700, Nepal
[b]Faculty, Department of Civil Engineering, Pulchowk Campus, Institute of engineering, Tribhuvan University, Lalitpur, 44700, Nepal
[c]Engineer, Ministry of Physical Infrastructure and Transport (MoPIT), Government of Nepal
Department of Civil Engineering Institute of Engineering, Thapathali Campus, Tribhuvan University, Kathmandu, Nepal, 44600

Abstract

The current study develops a three-dimensional FEM-based for geosynthetically stabilized flexible pavements, using PLAXIS 3D simulations supported by laboratory and field data. In particular, the effect of geogrid strengthening is considered for California Bearing Ratio (CBR) ranging from 5 to 15 and the loadings varying between 5 and 30 million standard axles (msa). Based on the simulation of biaxial geogrid with axial stiffness of 700 kN/m, the analysis determines the optimal location of the grid at the subgrade-subbase interface (100% of the base thickness) in order to minimize the vertical compressive strain at the subgrade level. As a result, considerable reduction in the base thickness can be achieved with the use of the suggested arrangement; in particular, the reduction is more than 100 mm (34%) for 30 msa at the weak subgrade (CBR 5-8) and 50-90 mm (10%-18%) for 20 msa loads. A design catalog developed within the scope of the investigation can serve as a valuable guide for engineers in optimizing pavement structure and extending the life of the pavement.

Keywords: Geogrid Reinforcement, Flexible Pavement Design, California Bearing Ratio (CBR), Finite Element Method (FEM), Service Life Ratio (SLR)

1. Introduction

The growing requirement for durable and economical road infrastructure construction under conditions of heavy traffic loading and difficult subgrades calls for advanced pavement design approaches. One of such approaches is the use of geosynthetics in flexible pavements where geogrids act as efficient pavement reinforcement material providing the improvement of load transfer, deformation decrease, and increasing the service life of the pavement. However, classical methods of design do not offer the necessary accuracy in taking into account the interaction of geogrids and other layers of the pavement. Numerical modeling, specifically Finite Element Method (FEM)-based one using software such as Plaxis 3D can be used to simulate real world conditions and estimate the advantages provided by reinforced pavement.

Numerical simulation plays a crucial role in the design of paved reinforced roads. Several simulations of the pavement model are conducted in order to investigate different scenarios and conditions, as shown in Table 1. It was possible to obtain some valuable information regarding several important parameters. The number of simulations conducted during the investigation is 405.

The main purpose of this research is to develop 3D FEM-based design guideline for geosynthetic stabilized flexible road pavements with emphasis on geogrids position optimization in order to improve pavement performance. The specific aims of the study include evaluation of service life, vertical strain reduction and saving in pavement thickness due to geogrid reinforcement. The scope of the research includes numerical modeling using Plaxis 3D, laboratory and field data.

1.1 Optimum Geogrid Placement

According to Perkins (2001) and Perkins and Ismeik (1997), one of the main conclusions derived from the simulation was the identification of the most appropriate location of geogrid in the pavement layer. Based on the analysis conducted, it can be concluded that the installation of geogrid between the subbase and subgrade layer will yield the most advantages in terms of reduction in the vertical stress and load transfer.

Corresponding author's email address: 079mstre001.aanchal@pcampus.edu.np

1.2 Enhanced Service Life

It was found that there was an increased life span of the pavement resulting from the use of geogrids. The analysis showed how the use of geogrids reduces the stress and strains caused by the load, hence lowering the probability of failure and increasing the life span of the pavement. This is especially significant in areas experiencing heavy traffic load (Nazzal et al. 2006; Al-Khateeb et al. 2011).

1.3 Reduction in Pavement Thickness

Other important findings included the maximum reduction in pavement thickness that could be attained through the use of geogrids. The findings showed that using geogrids would make it possible to have pavements with reduced thickness without compromising structural integrity. Such a practice would save money in terms of material and construction costs (Gao et al. 2019; Saad et al. 2005).

1.4 Development of a Design Catalogue

Based on the findings from the simulations, a new design catalogue was developed specifically for geogrid-reinforced flexible pavements. This catalogue provides detailed design guidelines and specifications, enabling engineers and designers to effectively implement geogrid technology in their projects. It serves as a practical reference for selecting appropriate materials, determining optimal geogrid placement, and assessing the expected performance benefits.

1.5 Comparison with Existing Catalogues

This study entailed the comparison between the newly proposed design catalogue through this research for reinforced pavements using geogrids and the existing design guidelines as stated in the Flexible Pavement Design Guide (FPDG, 2021) for unreinforced pavements. This comparison highlights the advantages of using geogrids, demonstrating that the performance metrics for geogrid-reinforced pavements surpass those of conventional unreinforced designs. It underscores the need for updated the current design methods by taking into account the geogrid technology to enhance pavement performance and sustainability. The resulting insights contribute to the advancement of pavement engineering, fostering the adoption of innovative materials and techniques to enhance road infrastructure (Abu-Farsakh et al. 2014; Abu-Farsakh and Chen, 2011; Ahirwar and Mandal, 2017; Bathurst and Naftchali, 2021; Calvarano et al. 2017; Indraratna et al, 2011; Leng and Gabr, 2005).

Table 1. Total number of finalized numerical models

CBR (%)	5 MSA	10 MSA	20 MSA	30 MSA
5-15	102	102	95	106

2. Soil investigated Site

Even though the design catalogue was formulated based on detailed parametric studies considering a large variety of subgrade and traffic conditions, field and lab testing was carried out at the Pulchowk site in order to develop a realistic base line for modeling (Figure 1).

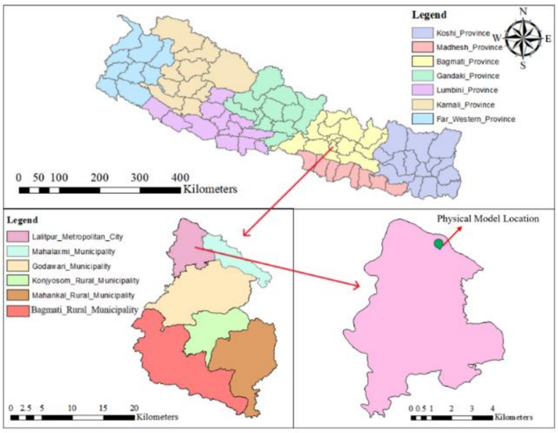

Figure 1. Soil investigated site for numerical evaluation (Coordinates: 27°40'59" N, 85°19'26" E)

The site data assisted in validating the appropriateness of the chosen material characteristics and modeling considerations under field conditions. The field test performed in this regard includes the DCPT, which is conducted to ascertain the in situ strength of the subgrade soil. Soil samples are collected from the subgrade soil and brought to the lab for performing various soil tests to determine its field CBR value, index properties, and compaction characteristics. The parametric study was carried out afterwards by varying the important parameters to values typical for Nepal. Hence, the design guideline that emerged is not site specific, but rather a generalized one, reflecting the pavement behavior under a wide range of engineering conditions.

3. Methods

3.1 Properties of subgrade materials

The properties of the subgrade materials are summarized in the following tables: Table 2 presents the gradation characteristics and Atterberg limits for Soil samples S1 and S2; Table 3 provides the Modified Proctor test parameters for both soils; and Table 4 details the CBR values corresponding to different dry densities achieved through varying compaction blows for (a) Soil S1 and (b) Soil S2.

Table 2. Gradation and Atterberg Limits of Soil S1 and S2

	Passing 75µm sieve (%)	Liquid Limit, LL (%)	Plastic Limit, PL (%)	Plasticity Index, PI (%)
S1	83.2	38.44	27	11.44
S2	82	30.47	26	4.47

According to Unified Soil Classification System (USCS), S1 & S2 both found to be ML (Inorganic silt, slight plasticity).

Table 3. Modified Proctor Test Parameters for Soil S1 and S2

	OMC (%)	MDD (gm/cc)
S1	15.8	1.74
S2	15.55	1.69

Table 4. CBR in Different Dry Density Maintained with Varying Blows: (a) of Soil S1 and (b) of Soil S2

	Dry density (gm/cc)	CBR
S1	2.01	13.33
	1.91	12.86
	2.04	14.29
	1.74	11.17
S2	1.70	9.71
	1.78	17.38
	1.72	13.81
	1.68	8.97

3.2 CBR from DCPT

DCPT DCPT data effectively complements laboratory CBR values by providing field-based insights into soil strength. Comp Field data obtained from DCPT test provide useful insights regarding the strength of soil compared with laboratory CBR values. Both approaches give additional insight for a better understanding of the load-bearing capacity of soil, hence increasing the reliability and accuracy of the geotechnical analysis. Field DCPT results can be used to calculate CBR using the equation developed by Kleyn and Van Heerden (1983), which is shown in Equation (1).

$$\text{Log CBR} = 2.628 - 1.273 \log(\text{DCP}) \tag{1}$$

Where, DCP = penetration mm/blow

Table 5. CBR from DCPT of sampling location S1 and S2

Depth	CBR (%) of soil sample, S1	CBR % of soil sample, S2
First 3m	25.28	17.79
Next 2m	7.58	8.19

Overall 5m	13.74	15.84

3.3 Direct shear tests

Direct shear tests indicated that Sample S1 had a cohesion of 45.4 kg/cm² and an internal friction angle of 12.84°, while Sample S2 showed a cohesion of 34.89 kg/cm² and a higher friction angle of 25.40°

3.4 Design of Reinforced Flexible Pavement

After conducting the laboratory test, pavement designing was done according to FPDG (2021), with the soaked CBR values and 20 million standard axle (msa) design traffic load. Three pavements were designed for comparison: (1) Unreinforced pavement as per the design from table 6; (2) Reinforced pavement of same thickness as that of unreinforced pavement (Table 7) in order to find out the effectiveness of the geogrid; and (3) Reinforced pavement of lesser thickness, which was optimized numerically (Table 8).

Table 6. Pavement design for unreinforced section to be used in numerical modelling

Unreinforced pavement section as per FPDG (2021)					
CBR	msa	GSB	WMM	Binder	Surface
10	20	150	150	0	60

Table 7. Pavement design for reinforced section without thickness reduction to be used in numerical modelling

Reinforcement in subgrade-subbase interface without thickness reduction						
CBR	msa	GSB	WMM	Binder	Surface	Geogrid
10	20	150	150	0	60	At 100%

Table 8. Pavement design for reinforced section with thickness reduction to be used in numerical modelling

Reinforcement in subgrade-subbase interface with thickness reduction						
CBR	msa	GSB	WMM	Binder	Surface	Geogrid
10	20	140	145	0	60	At 100%

The purpose of this study is to give efficient and sustainable pavements that are based on traffic loadings and type of soils. With the help of the right design procedures and laboratory and field test data, efficiency and sustainability of pavements could be improved. Among the design parameters used, average CBR of 10% that is based on samples collected from two sites is one and will be used to design thickness of the layers based on subgrade conditions. Another important design parameter used is the traffic loading of 20 million standard axles (msa) as recommended by DoR. Specifications of layers used in designing each pavement are as given in Table 9. Number of designs is as given in Table 10.

Table 9. Detail parameters of numerical model of pavement sections

Item	Description
Identification	National Highway
No. of Lanes	2
Traffic load (msa)	20
Total Pavement Width (m)	8.5
Carriageway (m)	7
Shoulder on Both Sides (m)	0.75
Pavement Extent (m)	10
Side Slope	2:1
Subgrade CBR (%)	10
Depth of GBS (mm)	150
Depth of WMM (mm)	150
Depth of DBM (mm)	0
Depth of AC (mm)	60

Table 10. Number of finalized numerical model run to assess the results

CBR%	5MSA	10MSA	20MSA	30MSA
5	12	11	11	12

6	12	12	12	12
7	11	12	11	12
8	11	11	11	12
9	11	12	11	10
10	11	10	9	12
11	11	11	10	12
12	11	11	10	12
15	12	12	10	12

3.5 Standard axle load configuration

Loading details are taken from IRC 37:2018 and its graphical representation are present in Figure 2.

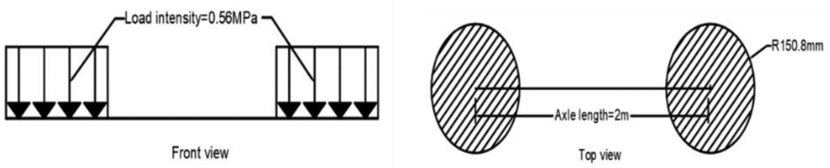

Figure 2. Wheel load configuration: Left Figure- front view showing loading intensity of tyre; Right Figure- top view showing contact area dimension

3.6 Properties of geogrid

For geogrid material, the axial stiffness is the ratio of the axial force F per unit width and the axial strain $(\Delta l/l)$ where Δl is the elongation and l is the original length):

$$EA = F/(\Delta l/l) \tag{2}$$

For isotropic material Shear stiffness (GA) can be computed according to the Reference Manual of Plaxis 3D (PLAXIS, 2024).

$$GA = EA/2 \tag{3}$$

The Lab test data from biaxial geogrid with stiffness of 700 kN/m corresponding to 2% strain is used for the analysis, and the material type is chosen as Elastic (Tables 11 and 12).

Table 11. Geogrid strength properties according to EN ISO 10319 ASTM D 6637

Testing method	EN ISO 10319:2015; ASTM D 6637: 2023
Geogrid type	40S
Tensile strength at 2% strain Longitudinal (kN/m)	14
Tensile strength at 2% strain Transverse (kN/m)	14
Stiffness calculated (longitudinal) (kN/m)	700
Stiffness calculated (transverse) (kN/m)	700

Table 12. Geogrid strength properties

Item	Description
Identification	Geogrid
Material type	Elastic
Longitudinal stiffness, EA1 (kN/m)	700
Transverse stiffness, EA2 (kN/m)	700
Shear stiffness, GA (kN/m)	350

3.7 Finite element modelling

Numerical model is prepared in PLAXIS 3D with the same geometry and layer properties of soil that was used in the physical model. Linear Elastic Model is adopted for the subgrade soil, granular layer and surface layer. Geogrid is modelled as surface element. Loading is assumed as of two point load each of 40kN each, applied on a single axle with a center-to-center wheel spacing of 2 m. The prepared numerical model is calculated and run to observe the strains, stress in the required locations. The wheel loads were applied in the traffic lane on the left side of the carriageway. After considering the effect of shoulder width, the left half of the cambered carriageway was considered, and the wheel loads were applied symmetrically about the center of the left half. This way of applying the loads was used to represent the actual wheel path of the vehicle.

3.8 Model geometry

The two lane road with a width of 3.5 m carriageway and 0.75 m shoulder for each lane results in a pavement width of 8.5m and its length is taken as 10m. Base, Subbase, DBM, AC layer thickness is taken into consideration as per the guidelines for the design of the flexible pavement as given by DOR in 2021(FPDG, 2021). However, in practical conditions, subgrade soil extends infinitely below the ground level but in the modelling process, its thickness is considered as 3m. This consideration of thickness is based on pressure bulb theory of Boussineq theory. Only 5.3 % of the total stress applied at the top surface gets transmitted to the bottom of 3m subgrade which is negligible.

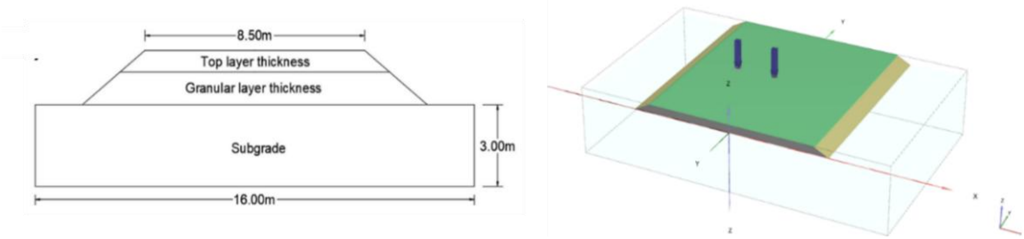

Figure 3. Detailing of model: Left Figure- sectional view; Right Figure- 3D view

According to IRC 37:2018, since it is assumed that the granular base and the granular subbase are taken as one layer while considering for analysis, the sum of thicknesses of both base and subbase is added and it is taken as one layer of granular material and one value of modulus is assigned to it. In the same way, for the purpose of analysis, DBM and AC is also taken as one layer. Creating an appropriate mesh of finite elements is an important step between creation of geometry and modeling of construction stages. For maintaining numerical stability and getting accurate results, it is important that the mesh is of good quality without having very thin or elongated elements. The PLAXIS 3D automatically creates the mesh depending on soil layers, structures, loads, and boundaries. Ten-noded tetrahedral elements are used for creating mesh (PLAXIS Reference Manual, 2024). The discretized model is shown in Figure 4.

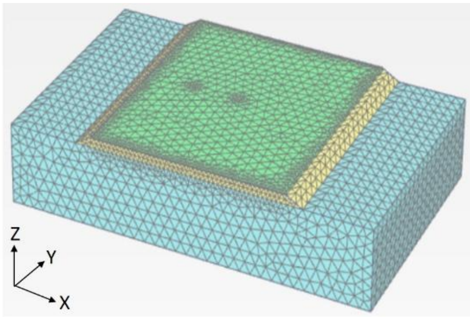

Figure 4. Connectivity plot of model geometry

3.9 Finite element analysis

During the analysis for the computation of the stresses and strains inside the model, each FEM software performs an iterative analysis with the aim of finding a solution which will satisfy the boundary conditions. Hence, the selection of the boundary conditions is very important in such a way that the displacements or strains on the boundary surface in all three directions must be true to the actual conditions at the site. The boundary conditions for the pavement model deformation and dynamics are shown in Table 13 and Table 14.

Table 13. Deformation Boundary Condition

Boundary	Condition
Boundary Xmin	Normally fixed
Boundary Xmax	Normally fixed
Boundary Ymin	Normally fixed
Boundary Ymax	Normally fixed
Boundary Zmin	Fully fixed
Boundary Zmax	Free

"Normally fixed condition" uses following criteria to set the boundary condition.

1. Vertical model boundaries with their normal in x-direction (i.e. parallel to the yz-plane), are fixed in x-direction (Ux=0) and free in y- and z-direction.
2. Vertical model boundaries with their normal in y-direction (i.e. parallel to the xz-plane), are fixed in y-direction (Uy = 0) and free in x- and z-direction.
3. Vertical model boundaries with their normal neither in x- nor in y-direction, are fixed in x- and y-direction (Ux = Uy = 0) and free in z-direction.

"Fully fixed condition" fixes the deformation in all direction and "Free" allows the deformation in all three directions.

Table 14. Deformation Boundary Condition

Boundary	Condition
Boundary Xmin	Viscous
Boundary Xmax	Viscous
Boundary Ymin	Viscous
Boundary Ymax	Viscous
Boundary Zmin	None
Boundary Zmax	None

"Viscous" condition absorbs all the outgoing wave energy and "None" condition applies only the standard fixity to the given boundaries.

Various sensors could be placed at mid-depth of base layer while constructing road model, and then strain, moisture content, and stress would be determined through the censors used after the application of an axle load of 80kN to the road model.

3.10 Optimum Position of Geogrid on Pavement

After the first phase of analysis on the performance of geogrids carried out in a pre-feasibility study, this research was focused on improving our understanding of the impact of the position of geogrids for the optimization of their performance in the pavement structure. We have systematically tested different locations within the granular layer of the pavement structure by changing the vertical position of the geogrids to maximize their reinforcing effect.

Trial 1 saw the geogrid being placed at 0% of the base thickness, which included the total thickness of the Wet Mix Macadam (WMM) base and Granular Base Subbase (GBS). This helped us establish the immediate performance of geogrid placement at the very bottom of the base layer.

Trial 2 entailed raising the position of the geogrid to 20% of the base thickness to find out if an increase in position would help distribute loads and reduce the stress concentration in the subgrade.

Trial 3 saw the geogrid being placed at 60% of the base thickness in order to allow us to determine the performance of geogrids when they were centrally located in the granular layer. In this trial, we expect that the position of geogrids will have been optimized in terms of reinforcing effect.

Trial 4 saw the geogrids being raised to 80% of the base thickness in order to establish if an elevation of the geogrid to this level would still have some performance benefit.

Finally, trial 5 entailed placing the geogrids at 100% of the base thickness.

Each of these trials was conducted with careful monitoring and analysis, with positioning details illustrated in Figure 5. This systematic approach allows for a comprehensive understanding of the geogrid's behavior across different depths, providing valuable insights into optimizing its placement for enhanced pavement performance.

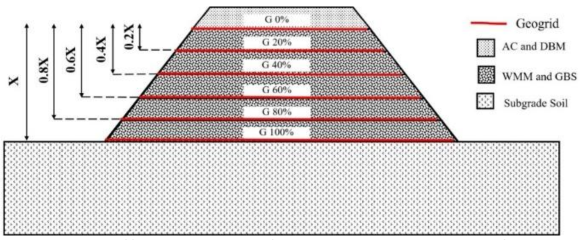

Figure 5. Different position of single layer geogrid used for analysis

For the biaxial geogrid having axial stiffness of 700 kN/m, tests were carried out using CBR ranging from 5 to 12 while keeping the same traffic load of 10 msa and other parameters fixed. The results, shown in Table 14 and Figure 6 below, demonstrate a definite possibility of decreasing the thickness of the pavement while retaining its service life. As verified through the simulations of PLAXIS 3D, reinforcement of the pavement using geogrid helps in decreasing the vertical strain on the top of the subgrade.

4. Results and Discussion

The findings from this study are consistent with the set objectives, and indicate that geogrid reinforcement plays a key role in the improved structural efficiency of flexible pavements. Through 3D finite element method analysis conducted by PLAXIS, the study establishes that the proper placement of geogrid layers at the subgrade and subbase interfaces reduces vertical strain, making it possible to minimize the base layer thickness while retaining pavement quality and lifetime. The design catalogue developed from this research work serves as an effective framework for utilizing geogrid technology. Table 15 below presents the % vertical strain reduction at the top of subgrade layer where geogrid is located at subgrade and subbase interface

Table 15. Percentage vertical strain reduction at the top of subgrade layer when geogrid is placed in subgrade-subbase interface

CBR	5 msa	10 msa	20 msa	30 msa
5	12.33	13.46	16.17	19.52
6	8.95	13.41	19.16	17.35
7	8.18	12.21	11.01	15.51
8	8.13	8.8	10.99	15.08
9	7.18	8.11	7.88	13.08
10	7.16	7.16	3.65	11.48
11	7.14	7.14	3.62	9.09
12	7.17	7.17	3.61	9.08
15	7.17	7.17	3.62	7.21

Furthermore, the study emphasizes the importance of continued exploration into the effects of geogrid placement on overall pavement performance, as well as its long-term benefits under varying environmental conditions. Therefore, further analysis of pavement with geogrid is carried out.

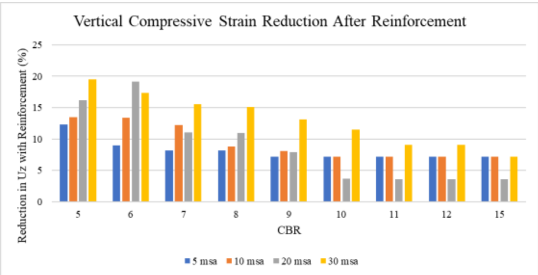

Figure 6. Vertical compressive strain (Uz) reduction at the top of subgrade

4.1 Optimum position of geogrid on pavement

Following the initial assessment of the efficiency of geogrid through pre-feasibility test, our study went ahead and sought to identify the best placement of geogrid for maximum efficiency. For this purpose, different placements were considered within the granular layer. In Trial 1, the geogrid was placed at 0% of the base thickness, where the base refers to the total thickness of the WMM base and GBS. In Trial 2, the geogrid was placed at 20% of the base thickness, in Trial 3 at 60%, Trial 4 at 80%, and Trial 5 at 100%, as per the parameters indicated in the previous section on performance analysis. Throughout this exercise, other parameters are maintained as is, with an axial stiffness of 700 kN/m biaxial geogrid being used. CBR varied from 5 to 12. The traffic load remained constant at 10 msa in all trials.

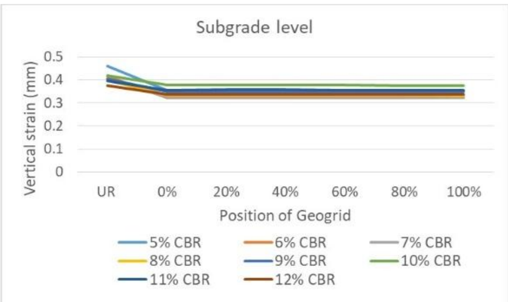

Figure 7. Vertical compressive strain produced at the top of the subgrade for varying CBR values under a 10 MSA traffic load

Trials were carried out to investigate the effect of various geogrid placements in the granular layer. It was observed that the optimum placement of the geogrid at 100% of the thickness of the base would result in the lowest vertical strain at the top of the subgrade. This would mean that the most effective geogrid placement would be at the subgrade-subbase interface and would be included in the design guidelines. Figure 7 depicts the effect of the vertical strain of the geogrid placement depth at various CBR levels. Figures 8-10 show the effect of geogrid reinforcement and subgrade CBR on the vertical compressive strain under the 10 MSA loading.

This important observation highlights the efficiency of installing the geogrid at the total thickness of the base, which demonstrates the most efficient application of the geogrid in reducing vertical strain on the flexible pavement structure. Not only do the findings prove the efficiency of the geogrid solution but they also give an important recommendation for the pavement design, highlighting the benefits of using geogrid in a systematic and comprehensive way. By applying geogrid, it becomes possible to spread loads throughout the pavement structure more evenly and avoid concentration of stresses in specific areas. Using geogrid also allows for increasing the durability of pavements and decreasing maintenance costs over the years. Therefore, when developing design recommendations, the geogrid is installed at 100% of base thickness (subgrade-subbase interface).

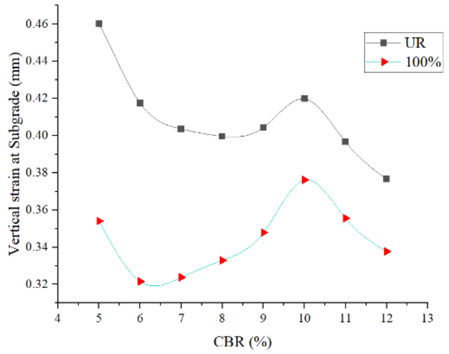

Figure 8. Strain comparison when geogrid is placed at 100% with that of unreinforced (UR) pavement

4.2 Thickness reduction of granular layer

After identifying the optimal geogrid position at 100% depth of the granular layer, a trial-and-error analysis was conducted to minimize the combined thickness of WMM and GBS layers. Using vertical strain at the subgrade top as a control parameter, the base thickness was gradually reduced—initially in 20 mm steps, then refined to 5–10 mm—until strain matched or slightly exceeded that of the unreinforced section. This process, applied across CBR values of 5–15 and traffic loads of 5–15 msa, produced optimized pavement sections detailed illustrated in Figure 9. The results confirm that geogrid reinforcement significantly enhances pavement performance while enabling material and cost savings, promoting both structural efficiency and sustainability in design.

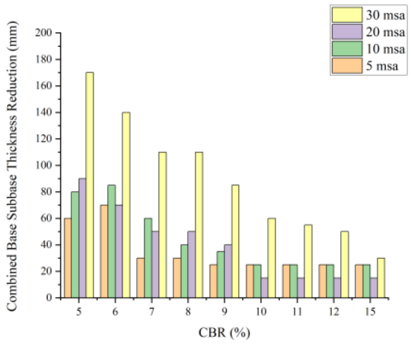

Figure 9. Reduction in granular layer thickness in mm after reinforcement

Based on numerical studies, it can be noted that the efficiency of geogrid strengthening grows with increased traffic load and decreased strength of the subgrade soil. For the considered range of traffic loads varying from 5 to 30 msa, considerable decreases in thickness of the granular layer have been found regardless of the value of CBR. The highest economy of materials was achieved for weak subgrades (CBR = 5-8%) - the savings varied from 12% to 34% for 30 msa and from 8% to 18% for 20 msa (Table 16).

Table 16. Reduction in granular layer thickness in mm after reinforcement (both mm and %)

CBR (%)	5 msa (mm / %*)	10 msa (mm / %)	20 msa (mm / %)	30 msa (mm / %)
5	60 / 12%	80 / 16%	90 / 18%	170 / 34%
6	70 / 14%	85 / 17%	70 / 14%	140 / 28%
7	30 / 6%	60 / 12%	50 / 10%	110 / 22%
8	30 / 6%	40 / 8%	50 / 10%	110 / 22%
9	25 / 5%	35 / 7%	40 / 8%	85 / 17%

10	25 / 5%	25 / 5%	15 / 3%	60 / 12%
11	25 / 5%	25 / 5%	15 / 3%	55 / 11%
12	25 / 5%	25 / 5%	15 / 3%	50 / 10%
15	25 / 5%	25 / 5%	15 / 3%	30 / 6%

4.3 Service Life Ratio

Service Life Ratio (SLR) is used in estimating the improvement in the service life of pavement through the use of reinforcement without altering the thickness of the pavement. SLR is defined as a ratio of service life of reinforced pavement to the service life of non-reinforced pavement under same loading conditions and same geometric characteristics. An increase in SLR indicates improved performance of the pavement by the process of reinforcement. Consistent with the Mechanistic-Empirical Pavement Design Approach in IRC: 37-2018, SLR was adopted in the current research to evaluate the performance of geogrid in improving the life of the pavement without changing the pavement thickness. SLR can be mathematically defined using vertical strain of pavement on subgrade as the ratio of the strain of non-reinforced pavement to the strain of reinforced pavement considering rutting and fatigue failure (Figure 10).

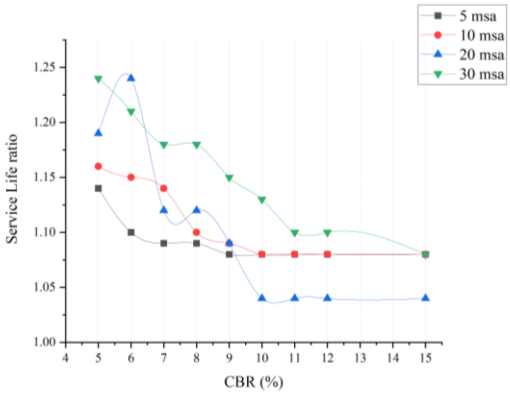

Figure 10. Service Life Ratio of flexible pavement for the subgrade of varying CBR values from 5% to 12% under traffic load of 5 MSA, 10 MSA, 20 MSA and 30 MSA when single layer geogrid is provided at 100% of base thickness compared with unreinforced pavement

4.4 Design Catalogue

A comprehensive design catalogue has been developed for CBR values ranging from 5 to 15 and traffic loads from 5 to 30 msa, as shown in Figure 11. It offers engineers a practical framework for geogrid-reinforced pavement design, comparing performance with conventional methods (FPDG, 2021). The catalogue highlights improvements in stability, load distribution, and reduced deformation. While it provides a strong foundation, site-specific factors must be considered. As a dynamic tool, the catalogue supports ongoing innovation, promoting sustainable and cost-effective pavement solutions.

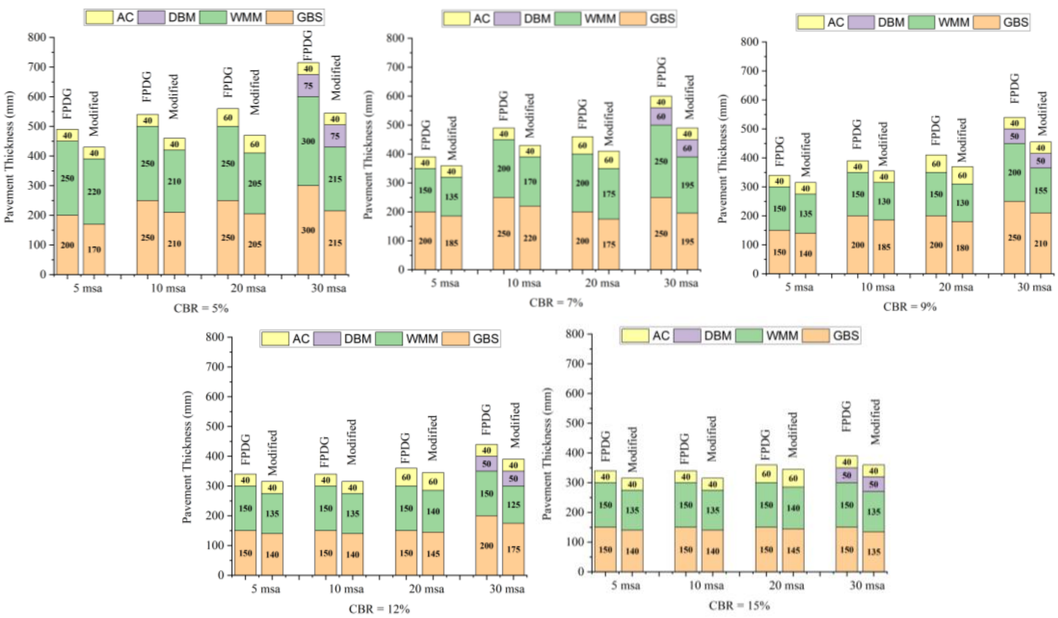

Figure 11. Catalogue for geogrid reinforced flexible pavement: Left Top Figure - CBR 5%; Middle Top Figure- 7% CBR; Right Top Figure- CBR 9%; Bottom Left Figure-CBR 12%; Bottom Right Figure- CBR 15%

The design catalog mentioned in Figure 11 clearly show the advantage that comes with the use of geosynthetics during pavement construction:

Reduction in thickness: For all CBR values (from 5-15%) and for all traffic loads (from 5-30 msa), the total pavement thickness in the case of the Modified design is smaller compared to the same value of thickness in the FPDG design. Therefore, the presence of geosynthetics contributes to the structural strengthening and allows decreasing the thickness of the granular and bituminous sections of the pavement structure.

Influence of traffic load (msa): With increasing the traffic load from 5-30 msa, there is an increase in the total thickness of the pavement. However, the difference between the thickness in FPDG design and in the Modified design becomes high with the increase in the traffic load. It means that geosynthetics provide an efficient way to deal with higher traffic loads.

Influence of subgrade strength (CBR):
Low CBR (5%): The thickness of the overall pavement is the largest one because of the weak subgrade.
High CBR (15%): The thickness of the overall pavement is the smallest one because of the strong subgrade.

Economic Effect: Since the stacked bars for the "Modified" design are shorter than those of "FPDG", the main conclusion to be drawn is that the use of geosynthetics reduces the necessary amount of material (AC, DBM, WMM, and GBS).

Thus, the above mentioned charts can be viewed as a design catalogue where it becomes evident that geosynthetic reinforcement is an effective replacement for some part of aggregate/bitumen, resulting in lighter pavements.

5. Conclusion and Recommendations

Conclusion

Results obtained from this research project provide clear evidence of significant reductions in vertical compressive strain and ability to achieve thickness reduction of pavements with geogrid reinforcement between subgrade and subbase. Important findings include:

- *Optimization of Design*: Modeling for CBR from 5 to 15 and traffic loads of up to 30 msa shows that the introduction of geogrid leads to effective optimization of pavement design. Optimal effects are provided for weaker subgrades under heavy traffic loads.
- *Performance of Low CBR Subgrades (CBR 5-8)*:
  - For 30 msa, the reduction in thickness of base layer exceeds 100 mm which constitutes 34% of the total thickness of pavement.
  - For 20 msa, thickness reduction from 50 to 90 mm was found which is about 10-18% of total thickness.
- *Performance of Higher CBR Subgrades (CBR 9-15)*: Thickness reduction varies from 15 to 85 mm providing 3%-17% improvement depending on the particular traffic load.
- *Structural Efficiency*: Such reductions are not accompanied by reduction in performance as the level of strain remains lower than in non-reinforced cases.
- *Practical Significance*: The results provide engineers with design table, which associates the benefits of geogrid introduction with particular subgrade strength and traffic.
- *Sustainability*: Overall, the research proves that geogrid introduction is a valid technique to increase structural efficiency and reduce cost of pavement construction.

Recommendations

- Implement Geogrid Implementation: Introduce geogrids at the subgrade-subbase interface level, particularly in cases of subgrades that have low CBR (5-8) and high traffic (up to 30 msa).
- Utilize the Design Catalogue: Implement the design catalogue produced in the research to ensure a systematic approach towards using geogrids for particular traffic and subgrade conditions.
- Practice Sustainable Construction: Practice geogrid reinforcement in order to save on costs and be material efficient without lowering effectiveness.

Acknowledgements

The authors would like to acknowledge the support extended and the resources made available through Research and Training Unit (RTU), Pulchowk Campus, Institute of Engineering, Tribhuvan University and Quality Research and Development Center (QRDC), Department of Roads, Government of Nepal. It is indeed praiseworthy the contribution made by the above mentioned authorities towards the completion of the present study. Specifically, the authors are grateful to Er. Hemant Tiwari (Society of Transport Engineers Nepal - SOTEN) and Er. Vibek Gupta (Safe and Sustainable Travel Nepal - SSTN) for their guidance and suggestions. The author would also like to remember staffs of Central Material Testing Lab (CMTL), and Heavy Lab. Pulchowk for facilitating various lab facilities and technical assistance during material testing.

References

Abu-Farsakh, M., & Chen, Q. (2011). Evaluation of Geogrid Base Reinforcement in Flexible Pavement Using Cyclic Plate Load Testing. *International Journal of Pavement Engineering*, 12(3), 275–288

Abu-Farsakh, M. Y., Gu, J., Voyiadjis, G. Z., & Chen, Q. (2014). Mechanistic–Empirical Analysis of the Results of Finite Element Analysis on Flexible Pavement with Geogrid Base Reinforcement. *International Journal of Pavement Engineering*, 15(9), 786–798

Ahirwar, S. K., & Mandal, J. N. (2017). Finite Element Analysis of Flexible Pavement with Geogrids. *Procedia Engineering*, 189(May), 411–416. Doi.org/10.1016/j.proeng.2017.05.065

Al-Khateeb, L. A., Saoud, A., & Al-Msouti, M. F. (2011). Rutting Prediction of Flexible Pavements Using Finite Element Modeling. *Jordan Journal of Civil Engineering*, 5, 173–190

ASTMD6637/D6637M - 15 (2023). Standard Test Method for Determining Tensile Properties of Geogrids by the Single or Multi-Rib Tensile Method.

Bathurst, R. J., & Naftchali, F. M. (2021). Geosynthetic reinforcement stiffness for analytical and numerical modelling of reinforced soil structures. *Geotextiles and Geomembranes*, 49(4), 921-940 Doi.org/10.1016/j.geotexmem.2021.01.003

BS EN ISO 10319 (2015). Geosynthetics - Wide Width Tensile Test

Calvarano, L. S., Palamara, R., Leonardi, G., & Moraci, N. (2017). 3D-FEM Analysis on Geogrid Reinforced Flexible Pavement Roads. *IOP Conference Series: Earth and Environmental Science*, 95, 022024

Federal Highway Administration (FHWA) (2015). Geosynthetic Design and Construction Guidelines

FPDG. (2021). Guidelines for the Design of Flexible Pavement (2nd Revision, 2021). Department of Roads (DoR), Ministry of Physical Infrastructure and Transport, Government of Nepal.

Gao, L.-S., Dan, H.-C., & Li, L. (2019). Response Analysis of Asphalt Pavement under Dynamic Loadings: Loading Equivalence. *Mathematical Problems in Engineering*, 1-15

Indraratna, B., Ngo, N. T., & Rujikiatkamjorn, C. (2011). Behavior of Geogrid-Reinforced Ballast under Various Levels of Fouling. *Geotextiles and Geomembranes*, 29(3), 313–322

IRC 37-2018 (2018). Guidelines for the design of flexible pavement; IRC: 37-2018 (4th Revision), Indian Roads Congress.

Leng, J., and Gabr, M. A. (2005). Numerical Analysis of Stress–Deformation Response in Reinforced Unpaved Road Sections. *Geosynthetics International*, 12, 111-119

Maccaferri products (2025). https://www.maccaferri.com [Last viewed on 15th Nov., 2025].

Nazzal, M., Abu-Farsakh, M., & Mohammad, L. (2006). Numerical Analyses of Geogrid Reinforcement of Flexible Pavements. In GeoCongress 2006: Geotechnical Engineering in the Information Technology Age; ASCE: Reston, VA, USA, 1–6

Perkins, S. (2001). Mechanistic-Empirical Modeling and Design Model Development of Geosynthetic Reinforced Flexible Pavements. Federal Highway Administration, Washington, DC, USA, 2001

Perkins, S., & Ismeik, M. A. (1997). A Synthesis and Evaluation of Geosynthetic-Reinforced Base Layers in Flexible Pavements-Part II. *Geosynthetics International*, 4, 605–621

PLAXIS. (2024). PLAXIS 3D Reference Manual. Bentley Systems Incorporated, Delft, The Netherlands.

Saad, B., Mitri, H., & Poorooshasb, H. (2005). Three-Dimensional Dynamic Analysis of Flexible Conventional Pavement Foundation. *Journal of Transportation Engineering* - ASCE, 131, 460-469

Tiwari, A., Shahi, P. B., Suwal, R., Tiwari, R. C., & Jha, P. K. (2025). Evaluating Geogrid-Reinforced Pavements with Field-Validated Soil Models under Vehicle Load Dynamics. *Journal on Transportation System and Engineering* 1 (2), 37-49